Control of a qubit under Markovian and non-Markovian noise

G. J. Delben,[1] M. W. Beims,[2] and M. G. E. da Luz[2,*]

[1]*Departamento de Ciências Naturais e Sociais, Universidade Federal de Santa Catarina, C. P. 101, 89520-000 Curitibanos-SC, Brazil*

[2]*Departamento de Física, Universidade Federal do Paraná, C.P. 19044, 81531-980 Curitiba-PR, Brazil*

(Received 25 April 2023; revised 12 July 2023; accepted 14 July 2023; published 31 July 2023)

An essential action in quantum information processing is the manipulation (control) of a single qubit, ideally a closed two-level system. However, in realistic applications, quantum processes are often under the influence of the external environment, e.g., presenting some degree of dissipation and decoherence. In this paper we address the emerging difficulties in the (tracking) quantum control of a two-level system under the influence of both Markovian and non-Markovian noise. We employ a same framework to treat both situations, a Lindblad-type equation, but considering that for the former (latter) case, the decay rate Γ is time independent (dependent). We discuss the conditions leading to a breakdown of the quantum control and eventual ways to overcome the problem, like employing a fast control scheme or controlling the off-diagonal terms of the system density matrix. Surprisingly, for Markovian noise such breakdown time decreases with Γ not as an exponential but as a power law. This indicates that the quantum control should be possible for a coupling between the system and the environment stronger than previously expected. Moreover, we find that for non-Markovian noise, the breakdown time is longer when there is backflow, i.e., $\Gamma(t)$ can be negative. The present theoretical results point to certain favorable scenarios to operate qubits even in a noisy medium.

DOI: 10.1103/PhysRevA.108.012620

I. INTRODUCTION

Tracking quantum control (QC) refers to making the quantum state (or specific observable expected values $\langle\mathcal{O}\rangle$) of a system to follow a predetermined chosen behavior. For instance, by means of well-tailored applied external field to drive the system evolution such that $\langle\mathcal{O}\rangle(t) = S(t)$, where $S(t)$ is a previously established trajectory. Mathematically, this constitutes an inverse problem, thus posing several fundamental and practical challenges (see, e.g., Refs. [1–10]).

Notably, QC protocols are better established for isolated (closed) than for nonisolated (open) systems. For a comprehensive discussion about the reasons for so as well as the limitations of certain formalisms in the literature we cite the reviews in [11,12]. Nonetheless, quantum open processes are unavoidable in many instances [13–17] and thus the QC must be implemented for systems which are actually coupled to the environment. In these cases, some general techniques are available like quantum error-correction schemes, optimal approaches, and structured pulse sequences [18–22]. Further works have also proposed distinct methods to minimize the effects of system-environment interaction by means of cooling, enhancement of quantum interference, diminishing of decoherence in parts of the full system, and decoupling the subsystems dynamics [23–32].

Among important applications demanding the QC of open systems we mention quantum computation [33–35]. Indeed, any conceivably quantum procedure aimed to manipulate information and then to release it to the classical world, as a "device output," should somehow display a determined degree of dissipation and decoherence [24]. Concretely, the primary unit of information at the quantum level is a qubit, a standard two-level system. Therefore, a basic operation in quantum information processing would be to manipulate an (ideally) isolated state $\rho = |\psi\rangle\langle\psi|$ for $|\psi\rangle = c_g\,|g\rangle + c_e\,|e\rangle$, where $|g\rangle$ and $|e\rangle$ are, respectively, the kets of ground and excited states (obviously, $|c_g|^2 + |c_e|^2 = 1$). But, it might be the case that ρ is not driven solely by unitary transformations. Interactions with the environment can impose dissipation and, even more drastically for quantum computation purposes [21,23], decoherence. Because of that, different studies (see below) have considered two-level open quantum problems, trying to understand the issues related to their QC.

The simplest kind of environment is when it is not sensibly affected by the system. Then, the action of the former on the latter does not depend on the previous temporal history of the mutual interaction. In such Markovian regime, the system "feels" the environment through a constant decay rate Γ, determining its quantum dissipation and decoherence. But distinct applications may demand QC at distinct scales of time, length, and energy. This can lead to a non-Markovian coupling [36], imposing extra difficulties for QC [11,37]. For example, recent investigations have focused on dephasing and thermal (thus non-Markovian) noise in qubits [38,39]. In these cases, a drastic shortcoming results from restrictions in arbitrarily populating the two levels: one is unable to vary $|c_e|^2$ in the entire range [0,1], precluding a full control of the qubit [40].

A common way to deal with this type of situation (open quantum systems) is to consider a straightforward, however very effective and handy, protocol [41,42]. One assumes a harmonic bath and then performs proper traces over the bath

*luz@fisica.ufpr.br

degrees of freedom. Hence, one gets a direct extension of the Liouville–von Neumann equation for $\rho(t)$. Actually, the final time-evolution formula has two extra simple terms depending on dephasing and thermal noise constant rates (see, e.g., [38,40]). Nevertheless, the construction has some restrictions, like to compute energy and heat fluxes, which would demand far more involved theories like hierarchical equations of motion (HEOM) [43–45].

In this paper we shall analyze the complications emerging in the tracking QC of a qubit under the influence of (i) Markovian and (ii) non-Markovian media. We discuss issues related to the breakdown time for the QC in terms of the problem parameters and address how to delay it by employing proper external control fields. In particular, we show that certain schemes of fast tracking QC can overcome different obstacles in driven a qubit. Moreover, we disclose certain trends in the QC due to memory effects associated with a non-Markovian environment.

We describe our two-level open system through a Lindblad-type master equation. The usual case of a constant decay rate Γ corresponds to (i). To model (ii), for the correlations having a finite time range, we heuristically rely on the framework in [46–48], for which the decay rate is assumed a time-dependent function $\Gamma(t)$. So, the non-Markovian character of the dynamics effectively occurs as a consequence of the exact time modulation of $\Gamma(t)$. In special, as highlighted in [46,47] a rich behavior arises when $\Gamma(t)$ can assume negative values and the divisibility of the evolution map does not hold true [48,49]. In connection to the QC protocol used here (the piecewise time-independent quantum control method, see below), the assumption of a $\Gamma(t)$ is based on a simple idea. The qubit continuously experiences the medium effects, but at short time windows δt_n, the medium is not considerably changed by the interaction. So, within δ_n the whole composed problem can be treated through the traditional Lindblad formalism [42], with a constant Γ_n. But due to the coupling, at successive time intervals the medium also goes through mild changes (a kind of thermalization). This should alter its influence on the system, accordingly generating $\{\Gamma_1, \Gamma_2, \ldots\} \to \Gamma(t)$. In this way, the profile of $\Gamma(t)$ could be viewed as resulting from a first-order linear response theory applied to the underlying non-Markovian quantum process [50–54].

To implement the tracking QC, the piecewise time-independent quantum control method (PTIQCM) [7,33,34,55] is particularly suitable. In fact, the PTIQCM has already been successfully used to explore different questions related to the control of qubits and qutrits [25,56,57].

The paper is organized as follows. In Sec. II we discuss the model construction for a qubit in the presence of Markovian and non-Markovian environments. We also briefly summarize the tracking QC scheme. In Sec. III we present our results and discussions. Significant attention is given to the breakdown of quantum controllability for a qubit in both types of environments. Final remarks are drawn in Sec. IV.

II. THE QC FRAMEWORK FOR A QUBIT

We suppose the following Hamiltonian:

$$\mathbf{H} = \mathbf{H}_S + \mathbf{H}_E + \mathbf{H}_I. \tag{1}$$

Here $\mathbf{H}_S = \mathbf{H}_0 + \mathbf{U}$ describes the qubit system S, i.e., the two-level $\mathbf{H}_0$ plus an applied potential $\mathbf{U}$, whose function is to drive the qubit. The term $\mathbf{H}_E$ represents the environment E and $\mathbf{H}_I$ gives the mutual interaction between S and E. Due to the characteristics and large size of the environment, $\mathbf{U}$ should not affect E. We also suppose $\{|g\rangle, |e\rangle\}$ the eigenstates of $\mathbf{H}_0$, with eigenfrequencies $\{\omega_g, \omega_e\}$ such that the natural transition frequency of S is $\omega_{eg} = \omega_e - \omega_g > 0$.

We consider that during the time interval $t_0 < t < T$, $\mathbf{U}$ results from an external monochromatic harmonic electric field applied to S in the dipole condition. Hence, in the basis of $\mathbf{H}_0$ one gets (for simplicity, with the field written in the complex form [58] and for $\tau = t - t_0$)

$$\mathbf{U}(t) = -\Omega_R \begin{pmatrix} 0 & \exp[i(\omega\,\tau - \varphi)] \\ \exp[-i(\omega\,\tau - \varphi)] & 0 \end{pmatrix}. \tag{2}$$

In Eq. (2) we have used the parametrization proposed in [34], with Ω_R, φ, and ω (all positive constants) being, respectively, the Rabi frequency (equal to the product of the moduli of the external field amplitude and the system dipole moment), the relative phase between the electric field and the dipole moment, and the external field frequency. The diagonal terms in Eq. (2) are null because the unperturbed states have defined parities, a typical situation for dipolar interactions. Further, $\Delta\omega = \omega - \omega_{eg}$ represents the detuning between the field and the system's natural frequency.

The density matrix $\rho(t)$ describes the full problem evolution, obtained from (for units where $\mu = \hbar = e = 1$)

$$i\frac{\partial}{\partial t}\rho(t) = [\mathbf{H}, \rho(t)]. \tag{3}$$

Tracing out over the environment variables, we get the subsystem reduced density matrix $\rho_S(t) = \mathrm{Tr}_E\{\rho(t)\}$. If S is in thermal equilibrium with E at $t = t_0$, then $\mathrm{Tr}_E[\mathbf{H}_E(t_0), \rho(t_0)] = 0$ and the reduced dynamical equation reads as [34,35] (with $\mathcal{L}$ the Liouville operator)

$$\frac{\partial}{\partial t}\rho_S(t) = -i\,[\mathbf{H}_S, \rho_S(t)] + \mathcal{L}\,\rho_S(t). \tag{4}$$

In the $\mathbf{H}_0$ basis we can write

$$\rho_S(t) = \begin{pmatrix} \tilde{\rho}_{gg}(t) & \tilde{\rho}_{ge}(t) \\ \tilde{\rho}_{eg}(t) & \tilde{\rho}_{ee}(t) \end{pmatrix}. \tag{5}$$

We assume that $\rho_S(t = t_0) = |\psi_0\rangle\langle\psi_0|$, with $|\psi_0\rangle$ being the system's initial state.

Under relatively natural assumptions [59], Eq. (4) can be cast as the Lindblad equation, or (with γ_0 a constant having units of inverse of time and thus Γ being dimensionless)

$$\frac{\partial}{\partial t}\rho_S = -i\,[\mathbf{H}_S, \rho_S] + \gamma_0\,\Gamma \times \frac{1}{2}\,(2\,\sigma_-\,\rho_S\,\sigma_+ - \sigma_+\,\sigma_-\,\rho_S - \rho_S\,\sigma_+\,\sigma_-). \tag{6}$$

For a time independent Γ, we have a constant spontaneous decay rate typifying a Markovian process. However, a possible realization for a non-Markovian bath can be obtained by simply assuming a decay rate which changes with time [36,37]. In this way, we can operationally set in Eq. (6) $\Gamma \to \Gamma(t)$ (for similar formulations see [48,60,61]). Without loss of

generality, in all which follows we suppose that numerically $\gamma_0 = 1$.

The motivation for this phenomenological ansatz is as following. Usually, when one considers a quantum mechanical decaying process due to a radiation field, represented by a structureless medium M constituted by a continuous of modes (the standard procedure in quantum optics [41]), first-order perturbation theory leads to $\delta C/C \sim -\gamma\,\delta t$. Here $|C(t)|^2$ is related to the probability of remaining in the initial excited state at time t and the constant $\gamma > 0$ is the spontaneous decay rate. This is a Markovian-type process since the variation δC, normalized by C, depends only on the time interval δt, but not on the exact time instant t. By operationally assuming $\gamma = \gamma(t)$ [and not $\gamma = \gamma(t, \rho_S)$ since S is too small compared to M], one is supposing that there is a type of reconfiguration of the medium M as a response to the interaction with the system, a mild relaxation. Now, the medium history (or memory feedback) is encoded into the integral $f(t) = \int_0^t dt'\,\gamma(t')$, such that $C(t) \sim C(0)\,\exp[-f(t)]$.

The above reasoning can be extended to the qubit embedding bath (representing the environment), so with Γ behaving like γ in the optical model. Moreover, the characteristics of this eventual non-Markovian process should naturally depend on the explicit functional form of $\Gamma(t)$ [62,63]. For instance, $\Gamma(t) \sim \exp[-t/\tau_0]$ would be related to a correlated bath, but of a finite timescale τ_0 [62]. On the other hand, $\Gamma(t) \sim \sin[\overline{\omega}\,t]$ [48] represents a process with an oscillating memory window. Note that in this last case we can have $\Gamma < 0$, meaning that in certain time intervals, instead of a decay, the environment provokes an enhancement of certain features of the system actual state [42]. These particular situations will be analyzed in Sec. III D.

A. Basic dynamical equations

In the great majority of works addressing open quantum systems, the control is performed considering the resonance case, namely, $\Delta\omega = 0$. The reasons for so are twofold [33,34,64,65]. First, in such condition, the energy transfer between field and system S is enhanced. Conceivably, this would help to drive the system to the excited state in shorter times, often a desirable feature in QC. Second, for $\Delta\omega = 0$ the equations are much easier to deal with, facilitating the calculations of the correct control parameter profiles. For completeness, we give an example of QC out of resonance in the Appendix A.

Hence, substituting Eq. (2) with $\omega = \omega_{eg}$ $(\Delta\omega = 0)$ into Eq. (6) and solving the resulting system of coupled differential equations (see [34]), for $t \geqslant t_0$ the exact expressions are $[\rho_{ge} = \exp[i\omega_{eg}\tau]\tilde{\rho}_{ge}, \rho_{ee} = \tilde{\rho}_{ee}, \bar{\Omega} \equiv \sqrt{64\Omega_R^2 - \Gamma^2}$, and the matrix elements at t_0 determined from $\rho_S(t_0) = |\psi_0\rangle\langle\psi_0|]$

$$\rho_{ee}(t) = \frac{4\Omega_R^2}{\Gamma^2 + 8\Omega_R^2} + \exp[-3\Gamma\tau/4]\,R_{ee},$$

$$R_{ee} = \left(\rho_{ee}(t_0) - \frac{4\Omega_R^2}{\Gamma^2 + 8\Omega_R^2}\right)\cos[\bar{\Omega}\tau/4] - \left[\mathrm{Im}\{\rho_{ge}(t_0)\exp[i\varphi]\}\,\frac{8\Omega_R}{\bar{\Omega}} + \left(\rho_{ee}(t_0) + \frac{12\Omega_R^2}{\Gamma^2 + 8\Omega_R^2}\right)\frac{\Gamma}{\bar{\Omega}}\right]\sin[\bar{\Omega}\tau/4], \tag{7}$$

$$\mathrm{Re}\{\rho_{ge}(t)\exp[i\varphi]\} = \mathrm{Re}\{\rho_{ge}(t_0)\exp[i\varphi]\}\,\exp[-\Gamma\tau/2], \quad \mathrm{Im}\{\rho_{ge}(t)\exp[i\varphi]\} = -\frac{2\Gamma\Omega_R}{\left(\Gamma^2 + 8\Omega_R^2\right)} + \exp[-3\Gamma\tau/4]\,I_{ge},$$

$$I_{ge} = \left(\mathrm{Im}\{\rho_{ge}(t_0)\exp[i\varphi]\} + \frac{2\Gamma\Omega_R}{\Gamma^2 + 8\Omega_R^2}\right)\cos[\bar{\Omega}\tau/4] + \left[\mathrm{Im}\{\rho_{ge}(t_0)\exp[i\varphi]\}\,\frac{\Gamma}{\bar{\Omega}} + \left(\rho_{ee}(t_0) + \frac{\Gamma^2 - 16\Omega_R^2}{4\Gamma^2 + 32\Omega_R^2}\right)\frac{8\Omega_R}{\bar{\Omega}}\right]\sin[\bar{\Omega}\tau/4], \tag{8}$$

$$\rho_{eg}(t) = \rho_{ge}^*(t), \quad \rho_{gg}(t) + \rho_{ee}(t) = 1. \tag{9}$$

Recalling that the expected value of any observable of the system (represented by a Hermitian operator $\mathcal{O}$) reads as

$$\langle\mathcal{O}\rangle(t) = \mathrm{Tr}_S\{\mathcal{O}\,\rho_S(t)\} \tag{10}$$

and that for $(i, j = e, g)$ $\langle i|\mathcal{O}|i\rangle = \mathcal{O}_i$ is real and $\langle i|\mathcal{O}|j\rangle = \mathcal{O}_{ij} = \mathcal{O}_{ji}^*$ $(i \neq j)$, we find from the expressions for the elements of ρ above

$$\langle\mathcal{O}\rangle(t) = (\mathcal{O}_g - \mathcal{O}_e)\,\tilde{\rho}_{gg}(t) + \mathcal{O}_e + 2\,\mathrm{Re}\{\tilde{\rho}_{ge}(t)\,\mathcal{O}_{eg}\}. \tag{11}$$

For instance, the reduced density matrix purity, which is a measure quantifying the degree of mixing of the qubit, yields [66] (using the relation between ρ_{ij} and $\tilde{\rho}_{ij}$ above)

$$P(t) = \mathrm{Tr}\left\{\rho_S^2(t)\right\} = \rho_{gg}^2(t) + \rho_{ee}^2(t) + 2\,|\rho_{ge}(t)|^2. \tag{12}$$

We also have the dimensionless energy (recalling that $\hbar = 1$) $\varepsilon_S(t) = \langle\mathbf{H}_S\rangle(t)/\omega_e = \langle\mathbf{H}_0\rangle(t)/\omega_e + \langle\mathbf{U}\rangle(t)/\omega_e = \varepsilon_0(t) + \Delta\varepsilon(t)$. Thus, by units of the excited state $|e\rangle$ energy, $\varepsilon_0(t)$ is the qubit energy and $\Delta\varepsilon(t)$ is a kind of "excess energy," i.e., beyond that necessary to excite the qubit, provided by the external field and hence available to be damped into the environment E. They read as

$$\varepsilon_0(t) = (1 - \omega_g/\omega_e)\,\rho_{ee}(t) + \omega_g/\omega_e,$$
$$\Delta\varepsilon(t) = -2\,(\Omega_R/\omega_e)\,\mathrm{Re}\{\exp[i(\varphi - \omega_{eg}\tau)]\,\tilde{\rho}_{ge}(t)\}. \tag{13}$$

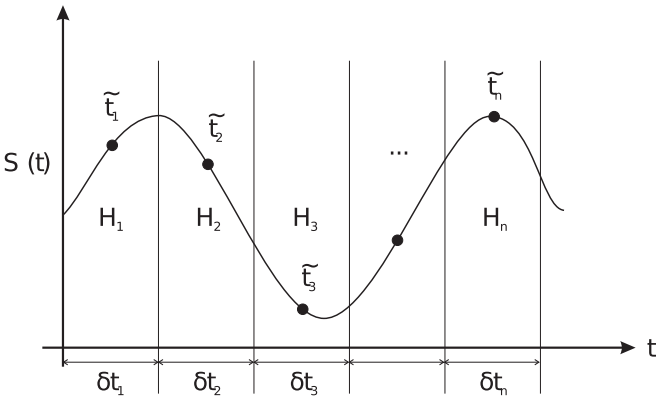

FIG. 1. Some aspects of the control procedure. The expected value $\langle \mathcal{O} \rangle(t)$ should follow a predetermined trajectory $S(t)$. The total Δt is divided into small time intervals δt_n. Within each δt_n, constant values for Ω_{Rn} and φ_n specify the subsystem Hamiltonian $\mathbf{H}_n(t) = \mathbf{H}_0 + \mathbf{U}(t; \Omega_{Rn}, \varphi_n)$. The parameters Ω_{Rn} and φ_n are then determined so that $\langle \mathcal{O} \rangle(\tilde{t}_n) = S(\tilde{t}_n)$. A proper choice for $\{\Omega_{Rn}, \varphi_n\}$ can make $\langle \mathcal{O} \rangle(t)$ to agree not only at the $\tilde{t}_n$'s, but also to be close to $S(t)$ in the entire Δt time interval.

Importantly for our later analysis, we observe from the above expressions that the "excess energy" is related to the off-diagonal term of the system S density matrix.

B. Control method

Essentially, the goal of any tracking control method is to employ a "tunable" external potential (applied to the original system H_0), so to obtain a specific expectation value for an observable of interest (frequently the eigenstate population). There are different ways to achieve this task [20,21,35,67]. For typical two-level quantum closed systems, a particularly simple and robust protocol is given in [7] (with a generalization to arbitrary N levels discussed in [55]). Such an approach has been adapted to open quantum problems in [34]. The procedure of [34], which we summarize below, is the one we are going to use throughout this work.

Suppose that during a time range $\Delta t = T - t_0$, we wish the expected value of an observable $\mathcal{O}$ to follow a predetermined trajectory $S(t)$ (e.g., that exemplified in Fig. 1). In other words, we shall properly drive S such that $\mathrm{Tr}_S\{\mathcal{O}\,\rho_S(t)\} = S(t)$. With this aim, the basic ingredients for the protocol in [34] are as follows (see Fig. 1):

(a) To divide Δt into small intervals $\delta t_n = t_n - t_{n-1}$.

(b) Within each δt_n to apply an external electric field of constant parameters values Ω_{Rn} and φ_n, obtaining a specific time evolution of $\rho_S(t)$ for $t_{n-1} < t < t_n$.

(c) In crossing the time intervals (i.e., at the t_n's), to quickly switch the field parameters value so that the sudden approximation, i.e., $\rho_S(t_n^+) = \rho_S(t_n^-)$, becomes valid. In practical terms, this means one to be able to change very rapidly the laser settings, a completely feasible task with the nowadays laser field technologies (see the detailed discussion in [7]).

(d) For every n, to select an instant $\tilde{t}_n$ within δt_n for which

$$\langle \mathcal{O} \rangle(\tilde{t}_n) = S(\tilde{t}_n). \tag{14}$$

The $\tilde{t}_n$'s exact values are not critically important provided the δt_n's are small enough [7]. Therefore, hereafter we will assume $\tilde{t}_n = t_{n-1} + \delta t_n/2$.

According to the above scheme, for each n we can take Eqs. (7)–(9) and (11) into Eq. (14), and thus to solve the resulting algebraic equation for Ω_{Rn} and φ_n. The obtained final $\{\Omega_{Rn}, \varphi_n\}$ (in the entire Δt interval) constitutes possible parameters set to perform the control.

As typical in control methods [7,21,68], at the different n's, we may get more than one solution for Ω_{Rn} and φ_n. This allows to look for a $\{\Omega_{Rn}, \varphi_n\}$ yielding a better implementation condition for the control, e.g., (i) a field with low amplitudes and (ii) parameter profiles with smoother variations along the δ_n's. In fact, it is even possible to construct a functional $h[\rho_S(t)]$ [34], and then to select just those $\{\Omega_{Rn}, \varphi_n\}$ minimizing $h[\rho_S(t)]$. In doing so, one can achieve QC by imposing a collection of restrictions to the dynamics. For example, in Ref. [34], the conditions were (ii) above as well as to maximize the system purity P [Eq. (12)]. We choose to perform the control looking for the smallest values for the Ω_{Rn}'s. In principle, this should be a proper condition from a practical point of view, e.g., minimizing the energy transfer to the environment.

We finally mention that if at a given δt_n there are no (or too high) Ω_{Rn} satisfying Eq. (14), it implies that the QC has been lost at the breakdown time $t_{\mathrm{bd}} = t_{n-1}$.

III. RESULTS AND ANALYSIS

To address the control of a qubit, we basically need to analyze the population of the excited state. Hence, in all the examples the observable is just the state projector $\mathcal{O} = P_e = |e\rangle\langle e|$, with $\langle O \rangle(t) = \rho_{ee}(t)$. For convenience, we often (but not always) adopt the same timescales employed in [34]. Thus, as done in [34] we plot the results in terms of the dimensionless time $\omega_0 t$. Note that so, in the absence of dissipation ($\Gamma = 0$), if the Rabi frequency had the value $2\,\omega_0$ (the assumed upper limit of Ω_R for the QC, see below), then one time unit would represent a full Rabi cycle oscillation. We numerically set $\omega_0 = \pi$.

In the simulations, we apply the control method described in Sec. II B, optimizing the control field parameters Ω_R and $0 \leqslant \varphi < 2\pi$. We recall that at each time step n, the protocol searches for distinct pairs (Ω_{Rn}, φ_n) satisfying Eq. (14) and selects that with the smallest value of Ω_{Rn}. Since we shall achieve the control from relatively low intensity fields, we restrict the maximum acceptable value for Ω_R. Thus, we assume that the QC has been "lost" at the breakdown time $t = t_{\mathrm{bd}}$ if to maintain the desired target trajectory $S(t)$, we must have $\Omega_R > 2\,\omega_0$ for $t > t_{\mathrm{bd}}$. Regarding φ, for all our examples next, after many exploratory simulations we have found that a value of $\varphi_n = 3\pi/2$, regardless of n and Ω_R, tends to yield a good QC (up to the breakdown time). Moreover, t_{bd} is fairly independent on φ. Thus, unless otherwise explicitly mentioned we choose $\varphi = 3\pi/2$, and in the control process only look for the appropriate Ω_R's. Also, we always take $-\omega_g = \omega_e = \omega_0/\pi$ and $\delta t_n = \delta t = 1/(5\,\omega_0)$.

Finally, an important aspect of the tracking QC is obviously the target trajectory $S(t)$. Its exact form will depend on the specific system, observable, and type of control one

TABLE I. The functional form of target trajectories $S(t)$ considered in this work and their particular interest (usefulness).

Interest	$S(t)$
Commonly used in the literature[a] to test tracking QC methods.	$(A/\pi)\arctan[\omega_0 t/\Lambda]$
Useful to test fast tracking QC schemes.	$B\,(\omega_0 t/\Lambda)^{\beta}$
Oscillates about the thermalization asymptotics, useful for prolonging the times for which $\rho_{ge} \neq 0$.	$(\omega_0 t/\Lambda')^{\mu}$, if $\omega_0 t < a$ $C\,\sin[\omega_0 t/\Lambda - b] + c$, if $\omega_0 t \geqslant a$

[a]See, for instance, Refs. [25,33,34,57].

shall perform (for an overview see, e.g., Ref. [69]). Here our interest is not in particular applications. Instead, we want to address certain general issues related to the QC of a qubit under a noisy environment. So, we suppose three "typical" $S(t)$'s, useful for distinct purposes. The first is commonly considered as a test trajectory in the development of tracking QC methods [25,33,34,57]. The second is a suitable profile to analyze fast control protocols (Sec. III C 1). The third has the proper shape to delay the vanishing of the off-diagonal density matrix elements (Sec. III C 2). They are summarized in Table I.

A. Performing the QC: A typical situation

We start with the first case in Table I (with $A = 2$ and $\Lambda = \pi$),

$$S(t) = \frac{2}{\pi}\arctan[\omega_0 t/\pi], \tag{15}$$

assuming the initial state

$$|\psi_0\rangle = |g\rangle. \tag{16}$$

In some of the examples next we suppose, on purpose, rather large (but constant, so Markovian) Γ values, e.g., 0.2. Such large decay rates are chosen precisely to increase the effects of decoherence in the system, so testing the limits of quantum controllability in extreme cases. We mention that in the literature Γ is usually much smaller, e.g., $\Gamma = \frac{1}{125}$ in [70].

In Fig. 2(a) we show the resulting control, i.e., the numerically obtained $\rho_{ee}(t)$ [which should follow as close as possible the target trajectory $S(t)$] and the quantities $|\rho_{ge}(t)|$ and purity $P(t)$ [Eq. (12)]. We notice a remarkably good control up to $t = t_{\rm bd}$ (in this case $t_{\rm bd} \approx 9/\omega_0$). As illustrated in Fig. 2(b), for $t > t_{\rm bd}$ we cannot find solutions for Eq. (14) such that $\Omega_R \leqslant 2\omega_0$. We also observe that $|\rho_{ge}|$ approaches zero for t tending to $t_{\rm bd}$. The same system and trajectory $S(t)$ have been discussed in [34] (see its Fig. 4). Here we have been able to maintain the control for a longer time (in Ref. [34] $t_{\rm bd} \approx 6/\omega_0$). Moreover, we get a higher purity near the $t_{\rm bd}$: $P(\omega_0 t = 6) \approx 0.5$ in [34] and $P(\omega_0 t = 9) \approx 0.68$ in Fig. 2. As it will be discussed later, these better outcomes (from a control point of view) are due to our choice of the Ω_R's, namely, to select the smallest possible values to implement the QC.

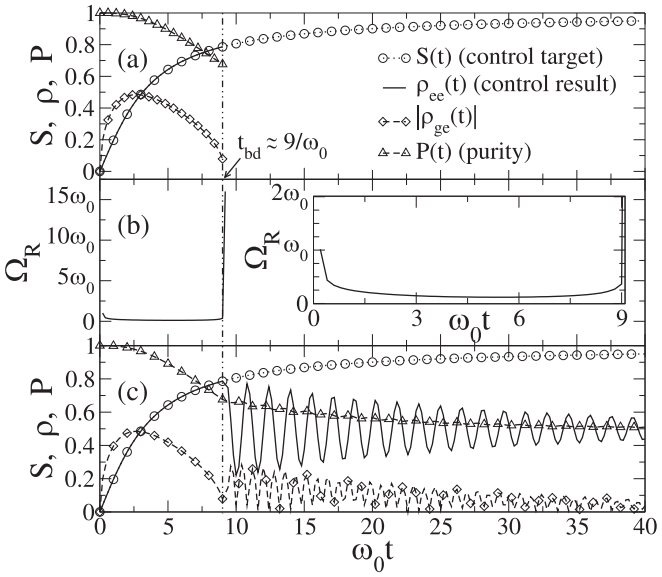

FIG. 2. (a) The achieved control for ρ_{ee} considering the target trajectory of Eq. (15) and $\Gamma = 0.2$. For the restriction of $\Omega_R \leqslant 2\omega_0$, the control is possible until $\omega_0 t \approx 9$, around which ρ_{ge} starts to vanish. The purity $P(t)$ decreases from 1 (at $t = 0$) to $P(t_{\rm bd}) \approx 0.68$. (b) The control parameter Ω_R profile, tending to diverge for $t > t_{\rm bd}$ (the inset presents Ω_R for t from zero to an instant at which $\Omega_R = 2\omega_0$). (c) The system full time evolution for $t \geqslant t_{\rm bd}$, where Ω_R is "frozen" to the value $2\omega_0$, evidencing the lost of the QC.

As mentioned above, by establishing an upper limit $2\,\omega_0$ for Ω_R, we cannot keep the QC beyond the breakdown time $t_{\rm bd}$ if $\Omega_R(t > t_{\rm bd}) \geqslant 2\,\omega_0$, as seen in Fig. 2(a). Nonetheless, we may ask what happens if at $t = t_{\rm bd}$ we just "freeze" $\Omega_R = 2\omega_0$ and then let the system to evolve. We present the corresponding dynamics in Fig. 2(c). Note that for $t > t_{\rm bd}$, the excited population $\rho_{ee}(t)$ displays damped oscillations towards $\rho_{ee} = \frac{1}{2}$, whereas $|\rho_{ge}(t)|$ initially mildly increases from

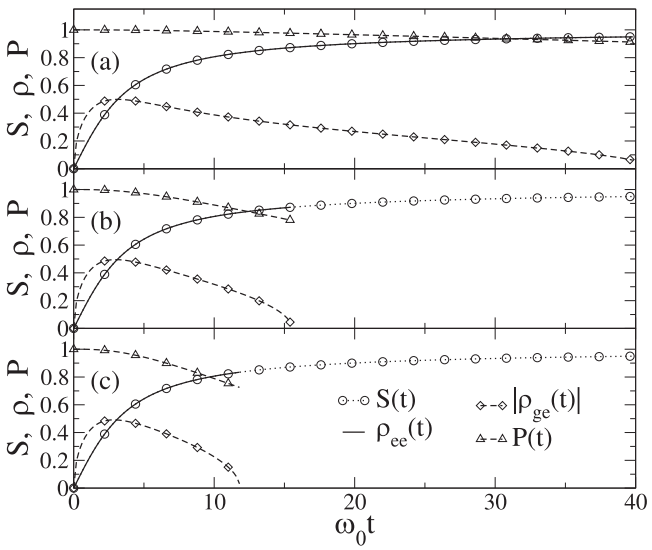

FIG. 3. The same as in Fig. 2(a), but for distinct values for the decay rate: (a) $\Gamma = 0.005$, (b) $\Gamma = 0.05$, (c) $\Gamma = 0.1$. The breakdown times are longer for smaller Γ's.

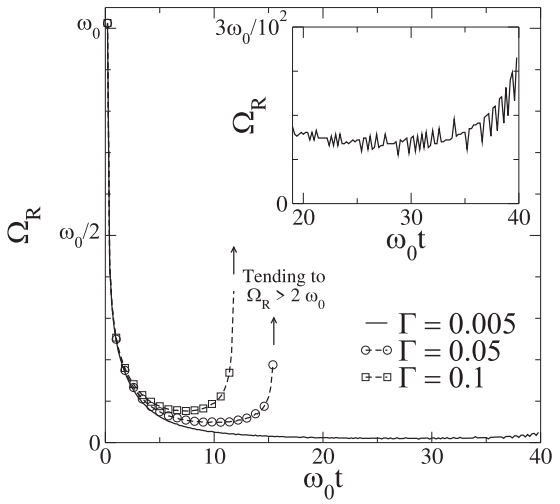

FIG. 4. The Ω_R profiles for the QC in Fig. 3. In the inset, a blowup of Γ_R versus t for the case of $\Gamma = 0.005$ in the time interval $20 \leqslant \omega_0 t \leqslant 40$.

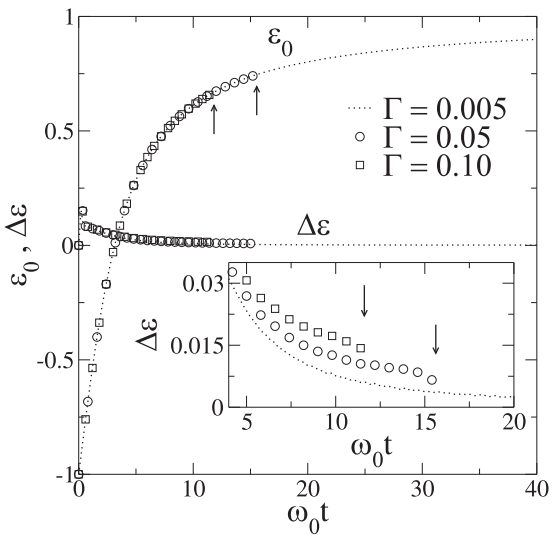

FIG. 5. For the QC in Fig. 3, the dimensionless energies ε_0 and $\Delta\varepsilon$ as function of $\omega_0 t$ for the three values of Γ. The inset shows blowups of $\Delta\varepsilon$. The arrows indicate the breakdown time, $\omega_0 t_{\rm bd} = 11.8$ ($\Gamma = 0.1$) and $\omega_0 t_{\rm bd} = 15.4$ ($\Gamma = 0.05$).

its $|\rho_{ge}(t_{\rm bd})|$ value, but eventually goes to zero as t increases. Further, the purity $P(t) \to \frac{1}{2}$ monotonically. Note that these results illustrate that by "quenching" the external control field in its configuration at $t = t_{\rm bd}$ does not help to extend the QC short after the $t_{\rm bd}$ [e.g., the drop in the $\rho_{ee}(t)$ from $t = t_{\rm bd}$ in Fig. 2(c) is very fast; the time interval for ρ_{ee} to reach the minimum value after $t = t_{\rm bd}$ is $\Delta t\, \omega_0 = 1$].

Compared to the literature, in the present example we have a reasonable increasing of $t_{\rm bd}$ (of 50% contrasted to that in [34]). However, independent on the method considered, the difficulty of maintaining the control in systems subjected to highly dissipative environments is well known [20,34,71]. As intuitively expected, the QC is easier to achieve for lower Γ's. We exemplify this by again considering the target trajectory in Eq. (15), and $|\psi_0\rangle = |g\rangle$, but setting three values for Γ, 0.005, 0.05, and 0.1. The obtained QC are shown, respectively, in Figs. 3(a)–3(c). Note that the breakdown time increases for decreasing Γ's. In all cases, ρ_{ge} is very small around $t_{\rm bd}$ (for more on this behavior, see below). Also, similarly to Fig. 2, the purity $P(t)$ decays with the time, with a rate which increases with Γ. In Fig. 4 we present the Ω_R profiles leading to Fig. 3. As it should be, for $t \lesssim t_{\rm bd}$, the necessary Ω_R to sustain the QC increases with Γ.

For the three QC examples in Fig. 3, we show in Fig. 5 the temporal variation of ε_0 and $\Delta\varepsilon$. We recall that ε_0 [function of ρ_{ee}, Eq. (13)] represents the energy of the qubit alone. Since in the three cases we are changing Γ but not the target trajectory $S(t)$, as it should be up to the breakdown time the ε_0 curves are exactly the same. Generally, the excess energy $\Delta\varepsilon$ [determined by ρ_{ge}, Eq. (13)], starts from zero at $t = 0$ (when $\rho_{ge} = 0$), rapidly raises to a maximum around 0.15, and then steadily decreases (following the trend of $|\rho_{ge}|$). From such maximum, the $\Delta\varepsilon$ curves gradually depart from each other, displaying greater values for larger Γ's. For details see the inset in Fig. 5. Our analysis confirms the intuitive expectation that more dissipative media tend to demand extra energy (apart from ε_0, quantified by a small $\Delta\varepsilon$) to implement the QC. But differently from the very sharp increasing of Ω_R, $\Delta\varepsilon$ approaches zero for $t \to t_{\rm bd}$. The point is that $\Delta\varepsilon$ depends on the product of Ω_R and $\mathrm{Re}\{\rho_{ge}\}$ and the latter seems to dominate near the breakdown time. These results indicate that ρ_{ge} and Ω_R are already good parameters to study the problem.

Relevant is how $t_{\rm bd}$ varies with Γ (assuming a constant decay rate). For instance, an exponential behavior $\omega_0 t_{\rm bd} \sim \exp[-c\,\Gamma]$ eventually would imply in only too low Γ's allowing reasonable long breakdown times. Obviously, the exact variation of $t_{\rm bd}$ with Γ should depend on the specific $S(t)$. Nonetheless, typical trends may result from typical goal trajectories. Therefore, for $S(t)$ in Eq. (15) and different values of A (refer to Table I) we have performed the QC for many different Γ's and then computed $t_{\rm bd}$ in each case. The curves $\omega_0 t_{\rm bd}$ versus Γ in a log-log plot are shown in Fig. 6. In each case we fit a power-law expression and determine the

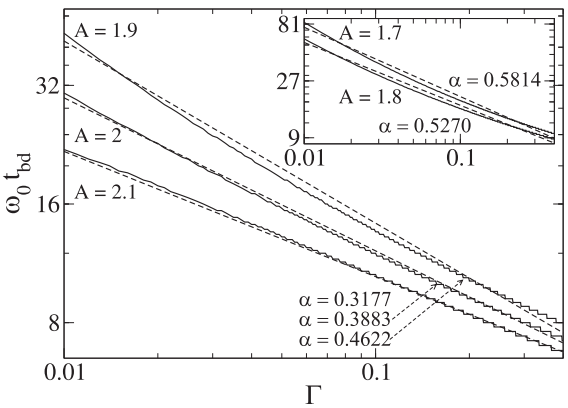

FIG. 6. Log-log plots of the control breakdown times as function of Γ, assuming the target trajectory in Eq. (15) with different values of A (see Table I) and $|\psi_0\rangle = |g\rangle$. The examples in Fig. 3 are for $A = 2$. The dashed lines are power-law fittings in the form $\omega_0 t_{\rm bd} \sim 1/\Gamma^{\alpha}$. The inset is just for a better visualization of the cases $A = 1.8$ and 1.7.

exponent α for $\omega_0 t_{\rm bd} \sim 1/\Gamma^\alpha$. We see fairly good agreements. In this way, differently from an exponential decay, acceptable $t_{\rm bd}$ might be possible even for larger values of Γ.

B. Factors involved in the QC breakdown

There are pertinent discussions in the literature about the difficulties of performing QC in open quantum systems (see the Introduction section). However, usually the focus is towards outlining the control breakdown [20,71] instead of identifying the reasons for so [11,72]. This is partially due to the involved methods used, powerful to implement the QC, but often not very practical to unveil subtle aspects of the system dynamics (as an example we can cite the sophisticated landscape optimal control protocol [73,74]). The control scheme employed here is straightforward, thus appropriate for investigating the conditions under which the QC can be lost. Hence, below we shall determine relevant factors resulting in the QC failure. But from the previous examples, two general trends seem to characterize the QC breakdown:

(a) $\rho_{ge}(t_{\rm bd})$ is always close to zero (cf. Fig. 3);

(b) $t_{\rm bd}$ is shorter for higher Γ's, conceivably following a power-law decay (Fig. 6).

So, consider the system "free" evolution (i.e., without any control) in which the field parameters are fixed. Then, $\rho(t)$ is determined by Eqs. (7)–(9). Due to the decaying exponential terms depending on Γ in such equations, the higher the Γ, the faster the (damped oscillatory) dynamics of $\rho_{ee}(t)$ and $\rho_{ge}(t)$ toward constant values. Indeed, for given Ω_R, φ, and $\Gamma \neq 0$ (all constants), a direct inspection in Eqs. (7)–(9) shows that asymptotically

$$\rho_{ee} \to A_{ee} = \frac{4\,\Omega_R^2}{\Gamma^2 + 8\,\Omega_R^2}, \quad \rho_{gg} \to \frac{\Gamma^2 + 4\,\Omega_R^2}{\Gamma^2 + 8\,\Omega_R^2}, \tag{17}$$

$$|\rho_{ge}| = |\rho_{eg}| \to A_{ge} = \frac{2\,\Gamma\,\Omega_R}{\Gamma^2 + 8\,\Omega_R^2}. \tag{18}$$

For the typical Γ's and Ω_R's considered, we have that $\rho_{ee}(t)$ [$|\rho_{ge}(t)|$] tends to a value close to $\frac{1}{2}$ (zero). For instance, for $|\psi_0\rangle$ the ground state, Eq. (16), and $\Omega_R = 1$ and $\varphi = 3\pi/2$, $\rho_{ee}(t)$ and $|\rho_{ge}(t)|$ are shown in Fig. 7. For the Γ's in Fig. 7, namely, 0.005, 0.05, 0.1, 0.2, the $t \to \infty$ limit of ρ_{ee} and ρ_{ge} are, respectively, 0.499 99 and 0.001 25, 0.499 84 and 0.012 50, 0.499 38 and 0.024 97, 0.497 51 and 0.049 75.

From these results, it becomes clear that any tracking QC goal, say, to make the matrix elements of $\rho(t)$ to follow specific target trajectories $S(t)$, forces an evolution which must *depart* or *deviate* from the problem asymptotic innate tendency, represented by Eqs. (17) and (18). This constitutes the great difficulty in controlling open quantum systems: The environment (by definition, unmanageable) imposes restrictions to what extent one might be able to drive the system observables by setting the external field parameters (within experimentally achievable possible values [26]). Therefore, a fundamental question is which are the actual mechanisms the control procedure should bypass, so to refrain (at least during a certain time period) the system natural evolution behavior.

To address the above, we observe that once we have the full set of parameters $\{\Omega_{Rn}, \varphi_n\}$ for the QC, the dynamics in each time window δt_n (see Fig. 1) is determined by Eqs. (7)–(9) using the corresponding pair (Ω_{Rn}, φ_n). Consequently, such

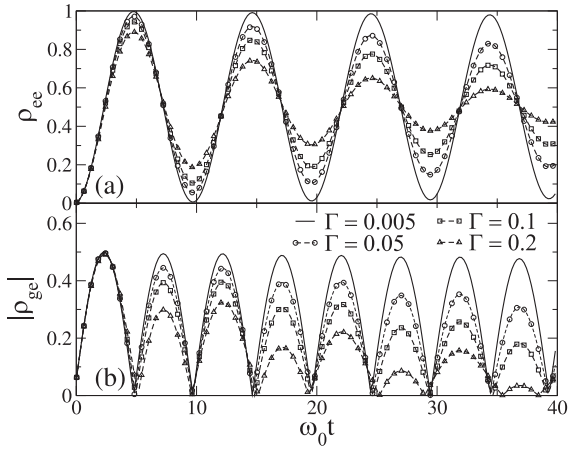

FIG. 7. The system time evolution without QC. It starts at the state $|\psi_0\rangle = |g\rangle$ with constant field parameters $\Omega_R = 1$ and $\varphi = 3\pi/2$. The plots show (a) $\rho_{ee}(t)$ and (b) $|\rho_{ge}(t)|$ for four distinct Γ values.

expressions may be seen as generating a map from one control window to the next. Thus, by defining

$$x_n \equiv \rho_{ee}(t_n^-; \Omega_{Rn}), \tag{19}$$

$$y_n \equiv \mathrm{Im}\{\rho_{ge}(t_n^-; \Omega_{Rn}) \exp[i\varphi_n]\}, \tag{20}$$

the rules $x_n \to x_{n+1}$ and $y_n \to y_{n+1}$ should correctly capture the QC dynamical trend and thus to help elucidating the reasons for the QC breakdown in the long term.

To derive the mapping, we can consider some simplifications in Eqs. (7) and (8), nonetheless maintaining their essential qualitative traits. First, we choose the δt's short enough so to guarantee a relatively smooth [compared to $S(t)$] set of $\langle \mathcal{O} \rangle(\tilde{t}_n)$ values [see Eq. (14)]. Second, in actual applications Γ is generally small and thus, in each time window, the decaying exponentials in Eqs. (7) and (8) can be fairly approximated to one. Third, $\Gamma/\bar{\Omega}$ is also very small and we can drop the terms multiplied by it. Then [$\delta t_n = \delta t$ and $f(\Gamma, \Omega_R) = (16\,\Omega_R^2 - \Gamma^2)/(16\,\Omega_R^2 + 2\,\Gamma^2)$]

$$x_{n+1} \approx \left\{ x_n \cos[\bar{\Omega}\,\delta t/4] + (1 - \cos[\bar{\Omega}\,\delta t/4])\,A_{ee} - y_n \frac{8\,\Omega_R}{\bar{\Omega}} \sin[\bar{\Omega}\,\delta t/4] \right\}\Big|_{\Omega_{Rn+1}}, \tag{21}$$

$$y_{n+1} \approx \left\{ y_n \cos[\bar{\Omega}\,\delta t/4] - (1 - \cos[\bar{\Omega}\,\delta t/4])\,A_{ge} + \left(x_n - \frac{f(\Gamma, \Omega_R)}{2} \right) \frac{8\,\Omega_R}{\bar{\Omega}} \sin[\bar{\Omega}\,\delta t/4] \right\}\Big|_{\Omega_{Rn+1}}. \tag{22}$$

Equations (21) and (22) already give us important information about the first steps of the QC evolution. We recall that often, the initial condition (at $t = t_0$) for the control is $|\psi_0\rangle = |g\rangle$, hence, $\rho_{ee}(t_0) = \rho_{ge}(t_0) = 0 \Rightarrow x_0 = y_0 = 0$. In this case, regarding the variation of Ω_R, Eqs. (21) and (22) display two distinct regimes at short and large times. Here we concentrate on the initial few control steps n. From Eq. (21) we see that the only term which can allow a considerable increase of x_{n+1} (compared to x_n) is that involving A_{ee} [cf. Eq. (17)]. Thus, at

the beginning Ω_R cannot be too small, as indeed observed in Figs. 2(b) and 4 for short t's. But then, for Ω_R increasing (yet, well below the established threshold), A_{ge} becomes very small and from Eq. (22) we see that for low n's, the most important contribution to y_{n+1} comes from the sine term. Accordingly, the successive first y_n's are negative (notice that the coefficient multiplying the sine function is initially negative).

On the opposite limit of larger n's, we note that term $\Gamma/\overline{\Omega}$ is generally very small and before the breakdown time the quantity $\overline{\Omega}\,\delta t/4$ is also small. So, expanding the cosine and sine functions and keeping only up to linear terms on their arguments, we find (for n big enough and defining $A_n = \Omega_{Rn}\,\delta t$)

$$\begin{aligned} x_{n+1} &\approx x_n - 2\,A_{n+1}\,y_n, \\ y_{n+1} &\approx y_n + 2\,A_{n+1}\,x_n - A_{n+1}. \end{aligned} \tag{23}$$

Two relevant facts can be inferred from Eq. (23). First, such map has a stable fixed point at $(x_n^*, y_n^*) = (\frac{1}{2}, 0)$, which agrees with the limits obtained from Eqs. (17) and (18) and represents the system natural "thermalization" asymptotics. Second, as one tries to increase the excited population (given by x_n) against the decaying effect from the environment, the off-diagonal term (given by y_n) evolves from negative values towards zero. But for $y_n \approx 0$, x_n ceases to increase and so the QC becomes impracticable. This explains why the control breakdown coincides with $|\rho_{ge}|$ going to zero.

We finally present a straightforward mathematical argument showing that higher Γ's yield shorter $t_{\rm bd}$'s. For so we revisit the derivation of Eq. (23) from Eqs. (21) and (22). Observe that the map in Eq. (23) does not depend on Γ. This is a consequence of (i) assuming $\overline{\Gamma}\,\delta t/4$ small and (ii) approximating $f(\Gamma, \Omega_R) \approx 1$ in Eq. (22). If we keep (i) but for (ii) set $f(\Gamma, \Omega_R) \approx 1 - 3\,\Gamma^2/(16\,\Omega_R^2)$, then the expression for x_{n+1} in Eq. (23) does not change. However, we gain the Γ-dependent *positive* term $3\,\Gamma^2/(16\,\Omega_R^2)A_{n+1}$ in the right-hand side of the expression for y_{n+1} in Eq. (23). Consequently, y_n (which is negative when n is small) will more rapidly converge to zero, implying in shorter breakdown times as Γ increases.

Lastly, we remark that from the present type of analysis, i.e., based on a discrete coupled map describing ρ_{ee} and ρ_{eg}, unfortunately we have not been able to analytically prove that $t_{\rm bd}$ decays as a power law of Γ. Nonetheless, all our numerical simulations point to such result.

Likewise useful is to preestimate which field parameter ranges could potentially increase the excited population ρ_{ee} above $\frac{1}{2}$ and to preclude ρ_{ge} from vanishing. As previously discussed, these are the system natural evolution trends which must be surmounted (at least temporarily), so allowing one to be able to implement the QC. To check this, for $0 \leqslant t \leqslant \delta t = 1/(5\,\omega_0)$ and $\Gamma = 0.2$ we display in Fig. 8 the dispersion of $\rho_{ee}(\delta t/2)$ and $|\rho_{ge}(\delta t/2)|$, i.e., their values in the middle of the time range, caused by distinct Ω_R and φ (maintained fixed in the entire time interval). We also assume two initial states $|\psi(t=0)\rangle = |\psi_0\rangle$. We see that $\Delta\rho_{ee}(\delta t/2)$, due to $\Delta\varphi$, is broader for greater Ω_R. Also, for any Ω_R, the maximum (minimum) $\rho_{ee}(\delta t/2)$ is achieved for $\varphi = 3\pi/2$ ($\varphi = \pi/2$). This is in opposition to the variation of $|\rho_{ge}(\delta t/2)|$ with φ. Hence, in trying to increase $\rho_{ee}(t)$ one tends to decrease $|\rho_{ge}(t)|$. From our mapping approximation description (see also Figs. 3 and 7), in the long run it leads to the tracking QC loss.

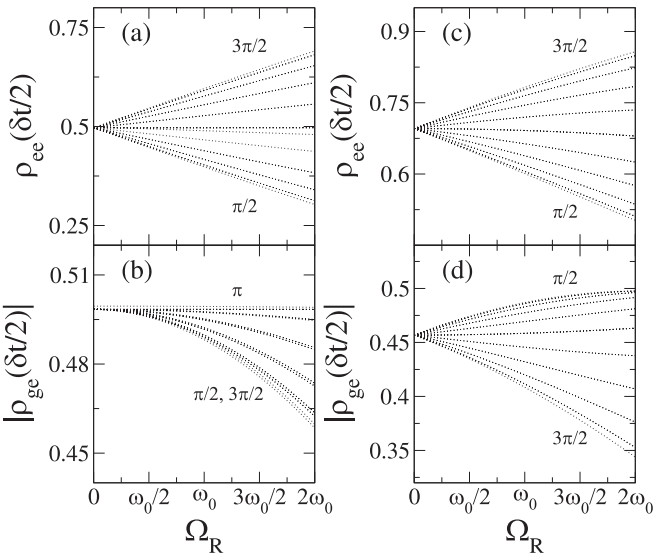

FIG. 8. The values of ρ_{ee} and $|\rho_{ge}|$ in the middle of the time interval $0 \leqslant t \leqslant \delta t$ as function of Ω_R. Here $\Gamma = 0.2$. Each curve represents a certain value of φ, whose minimum and maximum are indicated. In (a) and (b) $|\psi_0\rangle = \frac{1}{\sqrt{2}}(|g\rangle + |e\rangle)$ [so that $\rho_{ee}(0) = 0.5$]. In (c) and (d) $|\psi_0\rangle = \sqrt{0.3}\,|g\rangle + \sqrt{0.7}\,|e\rangle$ [so that $\rho_{ee}(0) = 0.7$]. In (b), the greatest values of $|\rho_{ge}(\delta t/2)|$ are obtained for $\varphi = \pi$.

We further perform akin investigations to those in Fig. 8, but now determining how the elements of $\rho(\delta t/2)$ depend on φ. For so, we fix $\Omega_R = 2\,\omega_0$. The results are depicted in Figs. 9(a)–9(d) for four different initial states. We notice that on the one hand $\rho_{ee}(\delta t/2)$, regardless of $|\psi_0\rangle$, has a maximum (minimum) at $\varphi = 3\pi/2$ ($\varphi = \pi/2$). On the other hand, the maximum and minimum positions of $|\rho_{ge}(\delta t/2)|$ can vary depending on $|\psi_0\rangle = c_g\,|g\rangle + c_e\,|e\rangle$, even exchange their locations, e.g., compare Fig. 9(a) with Fig. 9(d). In fact, for $|c_g|^2 > |c_e|^2$, $|\rho_{ge}(\delta t/2)|$ is generally smaller (larger) for $\varphi < \pi$

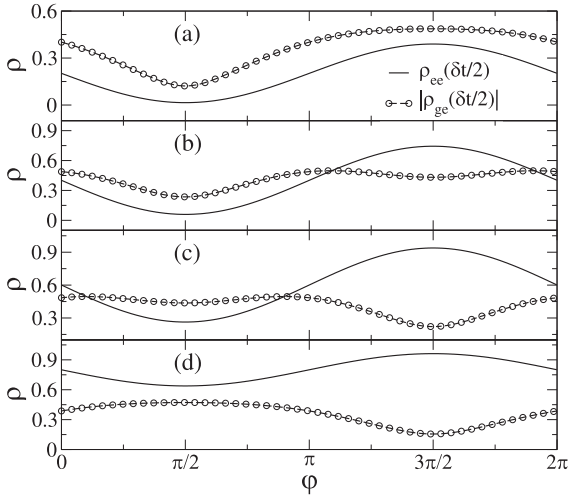

FIG. 9. Similar to Fig. 8, but now for fixed $\Omega_R = 2\,\omega_0 = 2\,\pi$ and the values of $\rho_{ee}(\delta t/2)$ and $|\rho_{ge}(\delta t/2)|$ given as function of φ. The initial states are (a) $|\psi_0\rangle = \sqrt{0.8}\,|g\rangle + \sqrt{0.2}\,|e\rangle$, (b) $|\psi_0\rangle = \sqrt{0.6}\,|g\rangle + \sqrt{0.4}\,|e\rangle$, (c) $|\psi_0\rangle = \sqrt{0.4}\,|g\rangle + \sqrt{0.6}\,|e\rangle$, (d) $|\psi_0\rangle = \sqrt{0.2}\,|g\rangle + \sqrt{0.8}\,|e\rangle$.

($\varphi > \pi$). Moreover, for $|c_{ee}|^2 < 0.5$ ($|c_{ee}|^2 > 0.5$), $\rho_{ee}(\delta t/2)$ and $|\rho_{ge}(\delta t/2)|$ display fairly similar (opposite) trends. The results in Fig. 9 point to a more diverse variation of ρ_{ee} and ρ_{ge} with φ, which is also dependent on $\rho(0)$. Thus, as we implement the control (and ρ and Γ_R change in time), the parameter φ should be much less critical for the QC outcomes as its influence (positive or negative) should be canceled out along the temporal evolution.

C. Overcoming the QC breakdown

The above discussions have pinpoint different aspects hindering the QC, which is invariably lost after a certain breakdown time $t_{\rm bd}$. So, a fundamental question is how to prolong it. Next we propose few ways to (at least partially) overcome some of the aforementioned issues.

1. Fast control

In certain schemes, like optimal control theory, one shall achieve a particular goal regardless the time (eventually long) it may take [26]. Conversely, there are situations where one needs to get to a final configuration as soon as possible. For instance, this might be necessary to minimize the effects of decoherence [26,28]. Then, a common procedure is to employ the so-called fast control protocol [75]. In our approach, if the aim is to have a specific final population and the trajectory $S(t)$ is not essential, we can choose a "faster" path, i.e., ensuring the same final population but in shorter times. As an illustration, consider to increase ρ_{ee} from zero to 0.9. Thus, we assume the second trajectory in Table I, with $B = 0.9$ and a rather large exponent $\beta = 8$, or

$$S(t) = 0.9\,(\omega_0\, t/\Lambda)^8. \tag{24}$$

By imposing $\rho_{ee}(t)$ equal to the above $S(t)$, at $\omega_0\, t = \Lambda$ the population of the excited state will be of 90%. However, initially the increase will be slow, starting to raise rapidly only for $\omega_0\, t$ close to Λ.

Assuming $S(t)$ in Eq. (15), for $\Gamma = 0.2$ the QC breaks down around $\omega_0\, t \sim 9$ for $\rho_{ee} \approx 0.8$ (refer to Fig. 2). In fact, for such $S(t)$ a very high population of $\rho_{ee} \approx 0.9$ has been reached only for $\Gamma = 0.005$ [at $\omega_0\, t = 20$, Fig. 3(a)]. For $|\psi_0\rangle = |g\rangle$, $\Gamma = 0.2$ and the trajectory of Eq. (24), we show in Fig. 10 the resulting QC for $\Lambda = 10, 20, 30, 40$. Note that for all the Λ's, the final goal has been attained (although for the latter two Λ's, $\omega_0\, t_{\rm bd}$ is just slightly above Λ). In particular, $\Lambda = 10$ is half the time taken in Fig. 3(a) to obtain a same population, even though in Fig. 10(a) the decay rate is 40 times larger than in Fig. 3(a). As for the purity $P(t)$, it practically equals to the unit up to $\omega_0\, t$ very close to Λ, when then $P(t)$ begins to drop (more sensibly for greater Λ's).

Figure 11 presents the field parameters necessary for the QC displayed in Fig. 10. We observe that Ω_R tends to be higher at $\omega_0\, t = \Lambda$ for shorter Λ's. But this an expected result since higher energies are generally required for shorter transition times. Nonetheless, even the highest Ω_R in Fig. 11, corresponding to Fig. 10(a), is about $1.1\,\omega_0$, therefore still relatively below our threshold limit of $2\,\omega_0$.

In Appendix B we present a similar analysis done in Fig. 6, i.e., discussing how $t_{\rm bd}$ varies with Γ, but now for $S(t)$ of the general form in Eq. (24). We corroborate our previous findings, namely, that $t_{\rm bd} \sim 1/\Gamma^{\alpha}$.

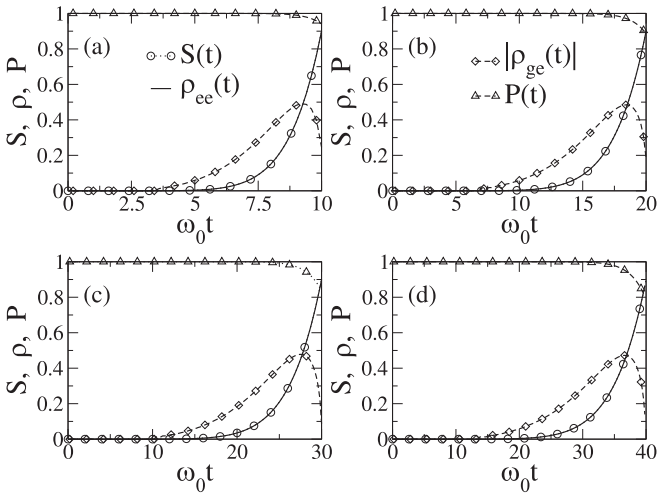

FIG. 10. The achieved QC for the target trajectory in Eq. (24) and $\Gamma = 0.2$. The values of Λ are (a) 10, (b) 20, (c) 30, (d) 40. In all cases the QC is sustained at least up to Λ, with $\rho_{ee}(\omega_0\, t = \Lambda) = 0.9$.

2. Controlling the off-diagonal density matrix elements

We have shown that a trend leading to the QC breakdown is $\rho_{ge}(t)$ to vanish along the process. Thus, we could try to prolong the control by delaying such tendency. However, this cannot be done for arbitrary tracking QC aims. Indeed, as discussed in Sec. III B, by driving $\rho_{gg} \to 0$ (so that ρ_{ee} steadily increases) we invariably get $\rho_{ge} \to 0$.

On the other hand, for paths where the populations fluctuate around a statistical mixture of g and e, say, with the purity varying around 0.5, conceivably we should have $\rho_{ge}(t) > 0$ for longer times and so $t_{\rm bd}$ would be extended. To confirm this, we suppose for $\rho_{ee}(t)$ the third target trajectory in Table I with $\mu = 1.865$, $\Lambda' = 5\,\pi$, $a = 11.2$, $C = 0.1$, $\Lambda = \pi/2$, $b = 6.8$,

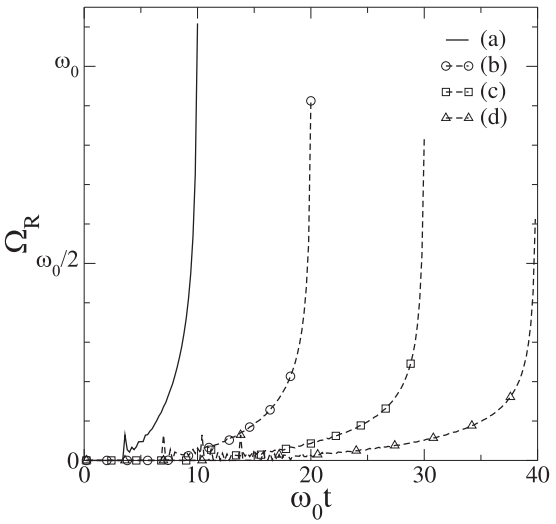

FIG. 11. The Ω_R profiles for the QC in Figs. 10(a)–10(d). The faster the population transfer (from ground to excited state), the greater the required Ω_R.

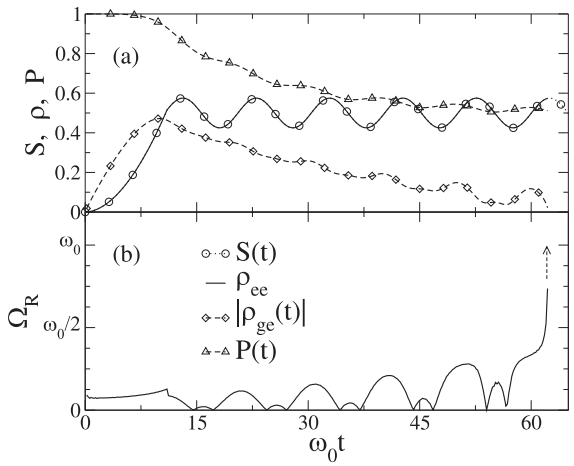

FIG. 12. (a) The QC of $\rho_{ee}(t)$ following the target trajectory in Eq. (25). For such $S(t)$, after some time $\rho_{ee}(t)$ must oscillate between 0.4 and 0.6. The associated $|\rho_{ge}(t)|$ and $P(t)$ are also shown. (b) The control parameter Ω_R profile. The arrow indicates that short after $\omega_0 t = 60$, to maintain the control, Ω_R should become larger than $2\,\omega_0$. Here $\Gamma = 0.2$.

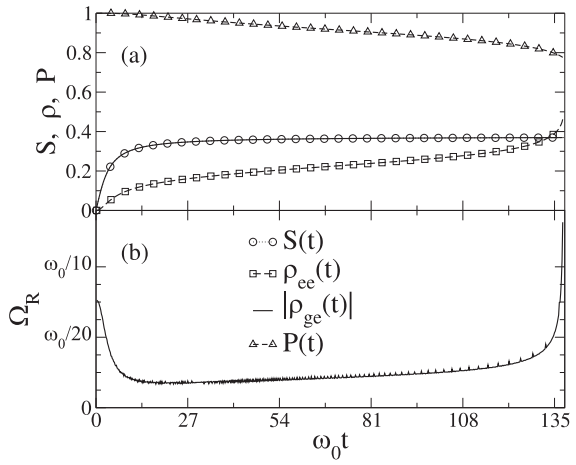

FIG. 13. For the target trajectory in Eq. (26), the resulting QC of $\mathrm{Re}\{\rho_{ge}(t)\}$ [so, in this case $\rho_{ee}(t)$ is not driven by the field, just evolving according to the system dynamics]. Here the initial state is $|\Psi_0\rangle = |g\rangle$ and $\Gamma = 0.2$. In the whole time interval considered, the purity $P(t)$ is never less than 0.8.

$c = 1/2$, thus,

$$S(t) = \begin{cases} (\omega_0 t/(5\pi))^{1.865}, & \omega_0 t < 11.2, \\ 0.1\,\sin[2\,\omega_0 t/\pi - 6.8] + 1/2, & \omega_0 t \geqslant 11.2. \end{cases} \tag{25}$$

Observe that after an initial linear ramp, $S(t)$ starts to oscillate between 0.4 and 0.6.

For our large $\Gamma = 0.2$, in Fig. 12 we display the obtained control. As in the previous examples, the QC is lost for ρ_{ge} tending to zero. But now this takes place for $\omega_0 t \gtrsim 60$, hence for a longer t_{bd}. Note also that $P(t)$ presents a slow decay from 1, with the QC breakdown coinciding with $P(t) \approx \frac{1}{2}$.

Until now we have always controlled the excited population, i.e., $\rho_{ee}(t)$. Alternatively, we can perform the QC for $\rho_{ge}(t)$. This certainly should extend the t_{bd}, but then the excited population will evolve according to the system resulting dynamics, no longer being the driven quantity. Such type of tracking QC may be of interest if the main objective is to maintain the qubit coherence (and not to have a very high population in the excited state), necessary in applications like implementing quantum gates, quantum cryptography, quantum teleportation, and quantum metrology [16,24,76]. So, in this case we set for Eq. (11) the matrix elements $\mathcal{O}_g = \mathcal{O}_e = 0$ and $\mathcal{O}_{ge} = \frac{1}{2}$, demanding that $\langle\mathcal{O}\rangle(t) = \mathrm{Re}\{\rho_{ge}(t)\} = S(t)$. As $S(t)$, we consider a temporal increasing similar to that in Eq. (15). Nonetheless, to impose too high values for $|\rho_{ge}(t)|$ usually leads to an earlier QC breakdown. So, akin to Eq. (15), but with a smaller prefactor A (Table I), we set

$$S(t) = \frac{0.375}{\pi}\,\arctan[\omega_0 t/\pi]. \tag{26}$$

The obtained QC is presented in Fig. 13. Note that the control is possible for relatively longer times than in the previous examples (here, $\omega_0\, t_{\mathrm{bd}} = 138$). For instance, at $\omega_0\, t = 137$ (thus, just before the t_{bd}) we have $|\rho_{ge}| = 0.37$ and $P = 0.78$. Furthermore, the purity $P(\omega_0 t \leqslant 90) \geqslant 0.9$. The population in the excited state, $\rho_{ee}(t)$, is not controlled. So, its raising tends to be slower. Even then, starting at $\rho_{ee}(0) = 0$, we get $\rho_{ee}(\omega_0 t = 137) = 0.44$. Finally, the necessary Ω_R for the control is rather low, increasing considerably only very close to t_{bd}.

D. Non-Markovian examples

Finally, we address some examples of a qubit under the influence of our phenomenological non-Markovian noise. To apply the PTIQCM, along each interval δt_n we assume $\Gamma(t) = \Gamma(\tilde{t}_n)$ (see Sec. II B). Hence, we can use the previous control equations, i.e., Eqs. (7)–(9), by just changing the values of the decay rate at the successive time windows: $\Gamma(\tilde{t}_n) \to \Gamma(\tilde{t}_{n+1})$ when $\delta_n \to \delta_{n+1}$.

For the numerical simulations, we again take $|\psi_0\rangle = |g\rangle$ and the target trajectory $S(t)$ in Eq. (15). Furthermore, unless for Γ, we suppose essentially the same parameter values used in Sec. III A (refer to Fig. 2) to control $\rho_{ee}(t)$. We discuss three $\Gamma(t)$'s investigated in the literature. An exponentially decaying profile [42]

$$\Gamma(t) = 0.2\,\exp[-\omega_0 t/\pi], \tag{27}$$

monotonically decreasing towards zero from its initial $\Gamma(0) = 0.2$ value. An exponentially decaying modulated shape [42]

$$\Gamma(t) = 0.2\,\sin[\omega_0 t/\pi]\,\exp[-\omega_0 t/(4\pi)], \tag{28}$$

for which $\Gamma(0) = 0$ and $\Gamma(t \to \infty) \to 0$. And a damped oscillating profile [77,78]

$$\Gamma(t) = 0.1 - 0.3\,\exp[-\omega_0 t/(5\pi)] \times (\cos[\omega_0 t/(2\pi)] + 0.2\,\sin[\omega_0 t/(2\pi)]), \tag{29}$$

for which $S(0) = -0.2$, $|S(t)| \leqslant 0.2$, and $S(t \to \infty) \to 0.1$. Importantly, complete positivity (CP) for the Lindblad equation can be ensured only when $\Gamma(t) > 0$ [46–49]. Hence, while for $\Gamma(t)$ in Eq. (28), CP is guaranteed just during the

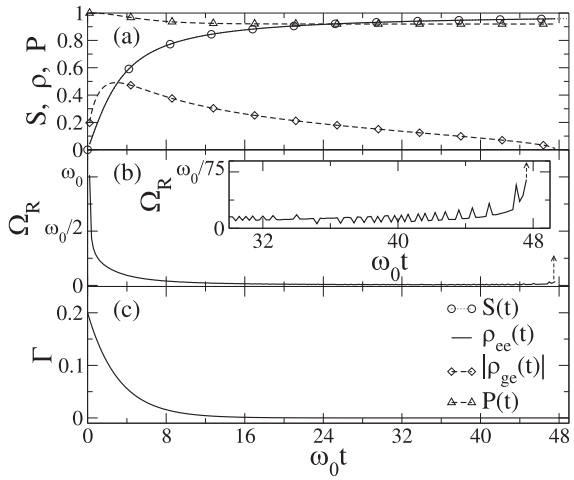

FIG. 14. (a) The controlled $\rho_{ee}(t)$ considering the target trajectory in Eq. (15) as well as the resulting $|\rho_{ge}(t)|$ and the purity $P(t)$. (b) The necessary Ω_R for the QC. The inset shows a blowup in the time interval $30 \leqslant \omega_0 t \leqslant 48$. The arrows indicate the instants in which Ω_R starts to increase very rapidly and thus the control is lost. (c) The profile of the time dependent $\Gamma(t)$ given in Eq. (27).

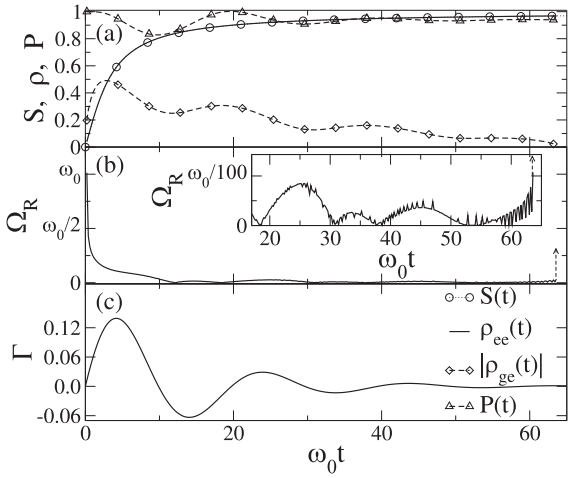

FIG. 15. Similar to Fig. 14, but for the time dependent $\Gamma(t)$ given by Eq. (28). The time intervals where $\Gamma(t) < 0$ correspond to the regions where $|\rho_{ge}(t)|$ and $P(t)$ increase.

time intervals $n\pi < \omega_0 t/\tau < (n+1)\pi$ $(n = 0, 2, 4, \ldots)$, for $\Gamma(t)$ in Eq. (29) this is always the case for $\omega_0 t > 7.6$.

Considering $\Gamma(t)$ in Eq. (27), the QC of $\rho_{ee}(t)$ is shown in Fig. 14(a) [for $\Gamma(t)$ refer to Fig. 14(c)]. Compared to Fig. 2, where $\Gamma = 0.2$ is a constant, for such monotonically decaying $\Gamma(t)$ the QC is attained for a much longer time, with the excited population reaching 95% at $\omega_0 t \approx 45$. Contrary to the purity function in the Fig. 2, which decreases from 1 (at $t = 0$) to about 0.7 (close to the breakdown time $\omega_0 t_{\rm bd} \approx 9$), here $P(t)$ is always above 0.9 in the entire control temporal range. Very emblematic is the fact the necessary Ω_R to maintain the QC decays similarly to Γ_R, as an exponential. Also, observe that after an initial increasing, $|\rho_{ge}(t)|$ starts to decrease, with $t_{\rm bd} \approx 47.6$, the instant in which ρ_{ge} vanishes.

For the $\Gamma(t)$ of Eq. (28), the control of $\rho_{ee}(t)$ is depicted in Fig. 15. Note that now $\omega_0 t_{\rm bd} = 63.6$, so longer than in the previous example of Fig. 14. To understand this, we observe that $|\rho_{ge}(t)|$ presents an overall decreasing trend, but with local growths in certain regions. Such behavior helps to postpone the QC breakdown. Note also that the time ranges where $|\rho_{ge}(t)|$ and $P(t)$ increase correspond to those for which $\Gamma(t) < 0$. Further, the shape of $\Omega_R(\omega_0 t > 10)$, Fig. 15(b) (recall that the parameter $\Omega_R \geqslant 0$), reflects the oscillations of the associated $\Gamma(t)$, Fig. 15(c).

As a last illustration, in Fig. 16(a) we show the QC of $\rho_{ee}(t)$ for the $\Gamma(t)$ in Eq. (29). The necessary Ω_R is depicted in Fig. 16(b). In the time interval where $\Gamma(t)$ is negative, $0 \leqslant \omega_0 t < 7.6$, $|\rho_{ge}(t)|$ displays a strong increase [see Fig. 16(a)]. Then, it starts to decrease only at $\omega_0 t \approx 21$, the instant corresponding to the maximum of $\Gamma(t)$, Fig. 16(c). In this way, the breakdown time of $\omega_0 t_{\rm bd} = 47.6$ in Fig. 14 should not be considered much longer than $\omega_0 t_{\rm bd} \approx 38$ in Fig. 16, especially by taking into account that $\int_0^{t_{\rm bd}} dt\, \Gamma(t)$ is 0.63 (2.94) for the former (latter) case. It is also relevant to observe that the purity remains practically one (a characteristic of closed systems) until extremely close to the breakdown time.

IV. FINAL REMARKS AND CONCLUSION

In this paper we have addressed the tracking control of a noisy qubit, described as a two-level system under the influence of Markovian and non-Markovian environments [this latter modeled through a heuristic time-dependent decay rate $\Gamma(t)$]. It is worth mentioning that tracking is a rather demanding type of QC. Indeed, other procedures, as the optimal control, have as the final goal to achieve a particular final state within a certain time period. In tracking QC, the aim is to impose observables or properties of interest, like coherence and purity, to follow a predetermined temporal evolution, usually specified by a target trajectory function $S(t)$. Such imposition is closely related to the process of manipulating more realistic (i.e., open) qubits for quantum processing purposes [21–24].

By means of comprehensive numerical simulations and analysis based on an approximated analytic map, describing the diagonal and off-diagonal terms of $\rho_S(t)$ [see Eqs. (19) and (20)], we have discussed the main aspects of the system dynamics. In particular, we have shown that the loss of the QC

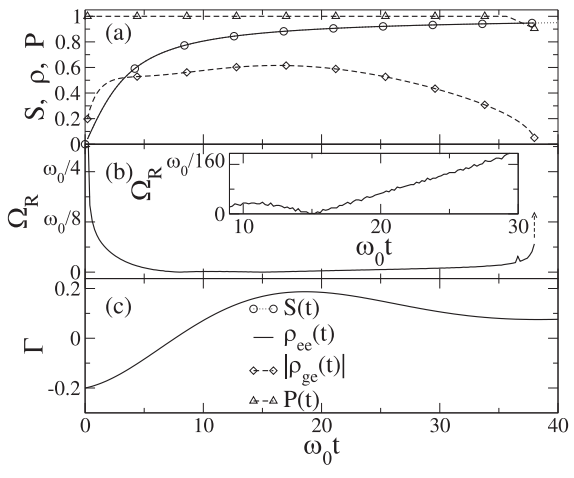

FIG. 16. Similar to Fig. 14, but for the time dependent $\Gamma(t)$ given by Eq. (29).

is due to intrinsic factors, inevitably making ρ_{ee}, $\rho_{gg} \to \frac{1}{2}$ and ρ_{ge}, $\rho_{eg} \to 0$ [in our mapping, this corresponds to the fixed point $(x_{n_{\rm bd}}, y_{n_{\rm bd}}) = (\frac{1}{2}, 0)$]. Moreover, the exact value of the breakdown time is related to how the characteristics of $\Gamma(t)$ (e.g., Γ positive and large) determine the evolution of $\rho_{ge}(t)$ towards zero.

Somehow surprisingly, we have unveiled that $t_{\rm bd}$ in the Markovian case goes as an inverse power law of the constant Γ, namely, $t_{\rm bd} \sim 1/\Gamma^{\alpha}$ with $\alpha > 0$. The exponent α depends on the problem parameters and control conditions, for instance, see the different numerical values for α in Fig. 6. Nonetheless, the important point is that this power-law trend seems to be general (as we have numerically tested for distinct situations, Fig. 6 as well as the Appendix B).

Also, few strategies to prolong the QC have been addressed. One is to follow fast control ideas [75], but here implemented in a different way, i.e., by means of an appropriate slope tunable (so potentially "faster") $S(t)$ [cf. Eq. (24) in Sec. III C 1]. Further, if the objective is not to have too highly excited populations (the typical aim in population inversion), instead of $\rho_{ee}(t)$ one may try to control the system density matrix off-diagonal terms. This possibility has been considered in Sec. III C 2, indeed leading to longer $t_{\rm bd}$'s.

Finally, we have investigated the tracking QC of a qubit in a non-Markovian medium, assuming that the non-Markovian effects are described by a phenomenological time dependent $\Gamma(t)$ [46–48]. We have supposed typical $\Gamma(t)$'s proposed in the literature [42,77,78]. We have found that the QC can be performed up to reasonable (i.e., not too short for eventual applications [13–17,35]) $t_{\rm bd}$'s. This demonstrates that a time dependence for the decay rate *per se* is not a problem to carry out tracking QC. In particular, we have confirmed previous speculations in the literature [12], proposing that the backflow of information [taking place when $\Gamma(t) < 0$] can help to maintain the QC.

As a last remark, the PTIQCM has been proven a good framework to study the QC of coupled qubits [56], certainly the required situation for actual quantum-information applications [16,19,24,55]. Hence, relying on the present results about the controllability of a single qubit under the influence of noise, a natural extension for our work is to employ the same scheme and assume the case of $\Gamma(t)$ for two or more interacting qubits. This is currently under investigation and it will be reported in due course.

ACKNOWLEDGMENTS

We are very grateful to W. T. Strunz for key valuable suggestions along different stages of this work. We also would like to thank G. M. Viswanathan for helpful discussions about Non-Markovian processes. M.G.E.L. and M.W.B. thank CNPq (Conselho Nacional de Desenvolvimento Científico e Tecnológico) for financial support (respectively, Grants No. 304532/2019-3 and No. 310294/2022-3). It is a pleasure to acknowledge support by the PROBRAL joint Brazilian-German program of CAPES (Coordenação de Aperfeicoamente de Pessoal de Nível Superior) and DAAD (Deutscher Akademisher Austauschdienst).

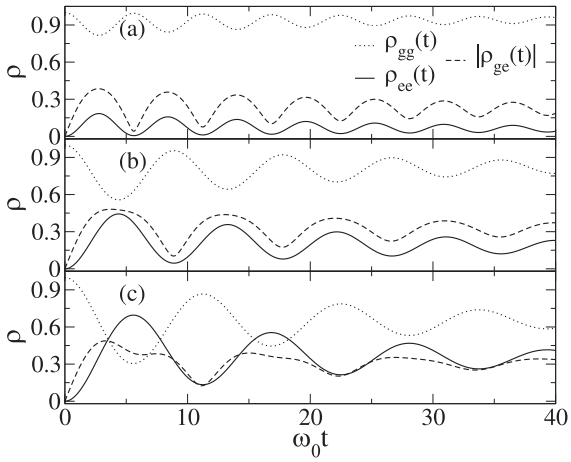

FIG. 17. Time evolution of $\rho_{gg}(t)$, $\rho_{ee}(t)$ and $|\rho_{ge}(t)|$ for fixed $\Gamma = 0.2$, $\Omega_R = \pi/4$, $\varphi = 3\pi/2$ and (a) $\Delta\omega = \omega_0$, (b) $\Delta\omega = \omega_0/2$, (c) $\Delta\omega = \omega_0/4$.

APPENDIX A: SYSTEM IN AN OFF-RESONANCE CASE $\Delta\omega \neq 0$

As discussed in Sec. II, in this paper our system has been analyzed assuming the resonance condition, i.e., $\Delta\omega = 0$. But of course, a pertinent query is whether or not the off-resonance case $\Delta\omega \neq 0$ would be more suitable to implement the QC. A relatively simple way to answer to this is to look at the system natural dynamics, namely, without applying any QC.

Since for $\Delta\omega \neq 0$ the resulting system of coupled differential equations (6) are very involved, we shall solve them numerically. For so, we consider the initial state $|\psi_0\rangle = |g\rangle$, a constant decay rate $\Gamma = 0.2$ and fix the external field parameters, with $\Omega_R = \pi/4$ and $\varphi = 3\pi/2$. By integrating the equations, we compute the temporal variation of $\rho_{gg}(t)$, $\rho_{ee}(t)$, and $|\rho_{ge}(t)|$.

In Fig. 17 we show the resulting evolution assuming three values for the detuning frequency: (a) $\Delta\omega = \omega_0$, (b) $\Delta\omega = \omega_0/2$, and (c) $\Delta\omega = \omega_0/4$. We clearly see that as $\Delta\omega$ increases, the range of variation of ρ_{ee}, and consequently of ρ_{gg}, decreases. Thus, larger detuning tends to restrict the population exchange between the fundamental and excited states. This certainly should restrict the possibility of making $\rho_{ee}(t)$ to follow an arbitrary target trajectory $S(t)$.

Therefore, we can conclude that the resonant case is the most appropriate for the tracking QC.

APPENDIX B: THE BREAKDOWN TIME VERSUS Γ FOR THE FAST CONTROL TARGET TRAJECTORY

For the target trajectory given in Eq. (24), we consider how $t_{\rm bd}$ varies with Γ for the same four values of Λ addressed in Fig. 10, namely, 10, 20, 30, and 40. The results are displayed in Fig. 18. We clearly see the same trend, $t_{\rm bd} \sim 1/\Gamma^{\alpha}$, as in Sec. III A, nevertheless for very small α's (the values are presented in Fig. 18). This is a consequence of the fact that for these examples, $S(t)$ displays a very slow initial increasing, being considerably different from zero only for $\omega_0 t$ close to Λ.

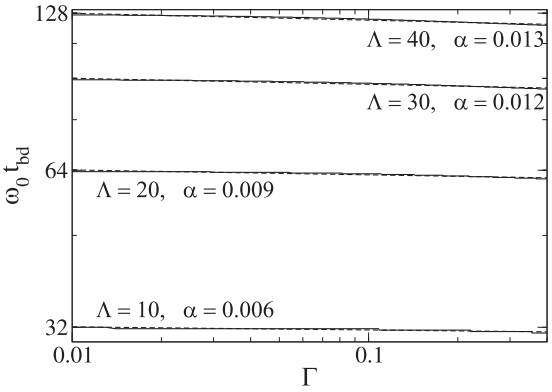

FIG. 18. The variation of $\omega_0\, t_{bd}$ with Γ for the same four parameter conditions of Fig. 10. The dashed lines represent fittings in the form $t_{bd} \sim 1/\Gamma^{\alpha}$.

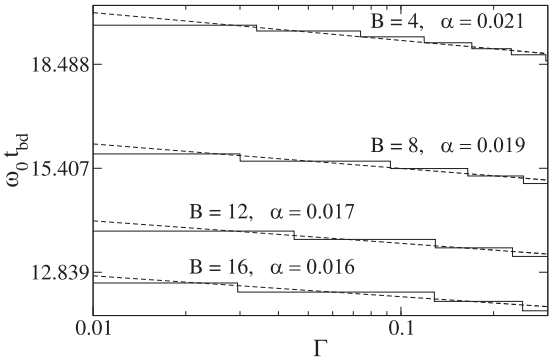

FIG. 19. Similar to Fig. 18, but for $S(t) = B\,(\omega_0\, t/10)^{3.5}$ and for distinct values of B. Again a fairly good fitting (dashed lines) is obtained from the general behavior $t_{bd} \sim 1/\Gamma^{\alpha}$.

For the same functional form of Eq. (24) with $\Lambda = 10$, but for $\beta = 3.5$ and four distinct values of B (see Table I), we perform the QC with $|\psi_0\rangle = |g\rangle$ and then determine the t_{bd} dependence on Γ. Note that now the raising of $S(t)$ is faster than in the previous case of $\beta = 8$. The obtained plots are depicted in Fig. 19. Once more the curves are well fitted by a power law. Also, the values of the exponents α here are a bit higher than in Fig. 18.

[1] D. J. Tannor and S. A. Rice, J. Chem. Phys. **83**, 5013 (1985).
[2] D. J. Tannor, R. Kosloff, and S. A. Rice, J. Chem. Phys. **85**, 5805 (1986).
[3] M. Shapiro and P. Brumer, J. Chem. Phys. **90**, 6179 (1989).
[4] B. Amstrup, R. J. Carlson, A. Matro, and S. Rice, J. Phys. Chem. **95**, 8019 (1991).
[5] R. S. Judson and H. Rabitz, Phys. Rev. Lett. **68**, 1500 (1992).
[6] H. Rabitz, R. de Vivie-Riedle, M. Motzkus, and K. Kompa, Science **288**, 824 (2000).
[7] J. Kuhn and M. G. E. da Luz, Phys. Rev. A **75**, 053410 (2007).
[8] C. Brif, R. Chakrabarti, and H. Rabitz, New J. Phys. **12**, 075008 (2010).
[9] N. Dudovich, D. Oron, and Y. Silberberg, Nature (London) **418**, 512 (2002).
[10] M. J. Calderón, B. Koiller, X. Hu, and S. Das Sarma, Phys. Rev. Lett. **96**, 096802 (2006).
[11] C. P. Koch, J. Phys.: Condens. Matter **28**, 213001 (2016).
[12] S. J. Glaser, U. Boscain, T. Calarco, C. P. Koch, W. Köckenberger, R. Kosloff, I. Kuprov, B. Luy, S. Schirmer, T. Schulte-Herbrüggen, D. Sugny, and F. K. Wilherlm, Eur. Phys. J. D. **69**, 379 (2015).
[13] Z. Amitay, A. Gandman, L. Chuntonov, and L. Rybak, Phys. Rev. Lett. **100**, 193002 (2008).
[14] T. Bayer, M. Wollenhaupt, C. Sarpe-Tudoram, and T. Baumert, Phys. Rev. Lett. **102**, 023004 (2009).
[15] D. Gerbasi, G. D. Scholes, and P. Brumer, Phys. Rev. B **82**, 125321 (2010).
[16] T. D. Ladd, F. Jelezko, R. Laflamme, Y. Nakamura, C. Monroe, and J. L. O'Brien, Nature (London) **464**, 45 (2010).
[17] J. Cai, G. G. Guerreschi, and H. J. Briegel, Phys. Rev. Lett. **104**, 220502 (2010).
[18] A. M. Steane, Phys. Rev. Lett. **77**, 793 (1996).
[19] E. Knill and R. Laflamme, Phys. Rev. A **55**, 900 (1997).
[20] H. Jirari and W. Potz, Phys. Rev. A **72**, 013409 (2005).
[21] M. Wenin and W. Potz, Phys. Rev. A **74**, 022319 (2006).
[22] G. S. Uhrig, Phys. Rev. Lett. **98**, 100504 (2007).
[23] J. Clausen, G. Bensky, and G. Kurizki, Phys. Rev. A **85**, 052105 (2012).
[24] E. Knill, Nature (London) **434**, 39 (2005).
[25] G. J. Delben and M. W. Beims, Phys. Scr. **96**, 025102 (2021).
[26] S. van Frank, M. Bonneau, J. Schmiedmayer, S. Hild, C. Gross, M. Cheneau, I. Bloch, T. Pichler, A. Negretti, T. Calarco, and S. Montangero, Sci. Rep. **6**, 34187 (2016).
[27] D. Girolami, Phys. Rev. Lett. **113**, 170401 (2014).
[28] X. Wang, M. Allegra, K. Jacobs, S. Lloyd, C. Lupo, and M. Mohseni, Proc. SPIE **10118**, 101180F (2017).
[29] L. Viola and S. Lloyd, Phys. Rev. A **58**, 2733 (1998).
[30] M. Wenin and W. Potz, Phys. Rev. A **78**, 012358 (2008).
[31] D. A. Lidar and S. Schneider, Quantum Inf. Comput. **5**, 350 (2005).
[32] J. Zhang, R.-B. Wu, C.-W. Li, and T. -J. Tarn, IEEE Trans. Automat. Contr. **55**, 619 (2010).
[33] L. G. C. Rego, L. F. Santos, and V. S. Batista, Annu. Rev. Phys. Chem. **60**, 293 (2009).
[34] C. A. Estrada Guerra, D. V. Villamizar, and L. G. C. Rego, Phys. Rev. A **86**, 023411 (2012).
[35] W. Zhu and H. Rabitz, J. Chem. Phys. **118**, 6751 (2003).
[36] I. de Vega and D. Alonso, Rev. Mod. Phys. **89**, 015001 (2017).
[37] W. Cui, Z. R. Xi, and Y. Pan, Phys. Rev. A **77**, 032117 (2008).
[38] D. Ran, W.-J. Shan, Z.-C. Shi, Z.-B. Yang, J. Song, and Y. Xia, Phys. Rev. A **101**, 023822 (2020).
[39] D. Ran, B. Zhang, Y. Chen, Z. Shi, Y. Xia, R. Ianconescu, and J. Scheuer, Opt. Lett. **45**, 3597 (2020).
[40] I. Medina and F. L. Semião, Phys. Rev. A **100**, 012103 (2019).
[41] H. J. Carmichael, *Statistical Methods in Quantum Optics 1, Master Equations and Fokker-Planck Equations* (Springer, Berlin, 1999).
[42] H. Breuer and F. Petruccione, *The Theory of Open Quantum Systems* (Oxford University Press, Oxford, 2002).
[43] A. G. Dijkstra and Y. Tanimura, Phys. Rev. Lett. **104**, 250401 (2010).
[44] A. Kato and Y. Tanimuera, J. Chem. Phys. **143**, 064107 (2015).

[45] P. P. Hofer, M. P. Llobet, L. D. M. Miranda, G. Haack, R. Silva, J. B. Brask, and N. Brunner, New J. Phys. **19**, 123037 (2017).
[46] H.-P. Breuer, E.-M. Laine, and J. Piilo, Phys. Rev. Lett. **103**, 210401 (2009).
[47] A. Rivas, S. F. Huelga, and M. B. Plenio, Phys. Rev. Lett. **105**, 050403 (2010).
[48] A. Pernice, J. Helm, and W. T. Strunz, J. Phys. B: At., Mol. Opt. Phys. **45**, 154005 (2012).
[49] V. Mukherjee, V. Giovannetti, R. Fazio, S. F. Huelga, T. Calarco, and S. Montangero, New J. Phys. **17**, 063031 (2015).
[50] H. Z. Shen, D. X. Li, and X. X. Yi, Phys. Rev. E **95**, 012156 (2017).
[51] M. Mehboudi, J. M. Parrondo, and A. Acín, New J. Phys. **21**, 083036 (2019).
[52] W. T. Strunz, Phys. Lett. A **224**, 25 (1996).
[53] L. Diósi and W. T. Strunz, Phys. Lett. A **235**, 569 (1997).
[54] W. T. Strunz, L. Diósi, and N. Gisin, Phys. Rev. Lett. **82**, 1801 (1999).
[55] G. J. Delben and M. G. E. da Luz, Quantum Inf. Process **15**, 1955 (2016).
[56] G. J. Delben, A. L. O. dos Santos, and M. G. E. da Luz, Phys. Rev. A **106**, 022417 (2022).
[57] A. L. O. dos Santos and G. J. Delben, Phys. A (Amsterdam) **574**, 126017 (2021).
[58] For mathematical simplicity, we represent the electric field as a complex wave, i.e., in the form $\varepsilon \exp[i\phi(t)]$ (ε eventually complex), instead of a real-valued function $\varepsilon \exp[i\phi(t)]+$ c.c. Considering the rotating wave approximation for the latter, the final expressions are the same as those obtained by using the former.
[59] G. Lindblad, Commun. Math. Phys. **48**, 119 (1976); V. Gorini, A. Kossakowski, and E. C. G. Sudarshan, J. Math. Phys. **17**, 821 (1976).
[60] H.-P. Breuer, B. Kappler, and F. Petruccione, Phys. Rev. A **59**, 1633 (1999).
[61] J. Piilo, S. Maniscalco, K. Härkönen, and K.-A. Suominen, Phys. Rev. Lett. **100**, 180402 (2008).
[62] G. M. Viswanathan, E. P. Raposo, F. Bartumeus, J. Catalan, and M. G. E. da Luz, Phys. Rev. E **72**, 011111 (2005).
[63] K. de Lacerda, L. R. da Silva, G. M. Viswanathan, J. C. Cressoni, and M. A. A. da Silva, Phys. A (Amsterdam) **597**, 127301 (2022).
[64] J. Eckel, J. H. Reina, and M. Thorwart, New J. Phys. **11**, 085001 (2009).
[65] N. Doslic, K. Sundermann, L. González, O. Mo, J. Giraud-Girardad, and O. Kühn, Phys. Chem. Chem. Phys. **1**, 1249 (1999).
[66] M. Schlosshauer, *Decoherence and the Quantum-to-Classical Transition* (Springer, Berlin, 2007).
[67] M. H. Goerz, D. M. Reich, and C. P. Koch, New J. Phys. **16**, 055012 (2014).
[68] A. Jha, V. Beltrani, C. Rosenthal, and H. Rabitz, J. Phys. Chem. A **113**, 7667 (2009).
[69] H. W. Wiseman and G. J. Milburn, *Quantum Measurements and Control* (Cambridge University Press, Cambridge, 2010).
[70] D. Dong, I. Petersen, and H. Rabitz, IEEE Trans. Automat. Contr. **58**, 2654 (2013).
[71] L. C. Wang, S. C. Hou, X. X. Yi, D. Dong, and I. R. Petersen, Phys. Lett. A **378**, 1074 (2014).
[72] I. Rotter and J. P. Bird, Rep. Prog. Phys. **78**, 114001 (2015).
[73] A. Pechen, D. Prokhorenko, R. Wu, and H. Rabitz, J. Phys. A: Math. Theor. **41**, 045205 (2008).
[74] A. Pechen and N. Il'in, J. Phys. A: Math. Theor. **50**, 075301 (2017).
[75] M. R. James, Annu. Rev. Control Robot. Auton. Syst. **4**, 343 (2021).
[76] L. Aolita, F. de Melo, and L. Davidovich, Rep. Prog. Phys. **78**, 042001 (2015).
[77] B. Bellomo, R. Lo Franco, and G. Compagno, Phys. Rev. Lett. **99**, 160502 (2007).
[78] A. C. S. Costa, M. W. Beims, and R. M. Angelo, Physica A (Amsterdam) **461**, 469 (2016).